Design Analyses Twist-Coupled Wind Turbine Blades

Shaik Wali
M.Tech,
Dept of Mechanical Engineering,
Syed Hashim College of Science &
Technology, Pregnapur, Medak District.

Mohd Mansoor Ahmed
M.Tech,
Dept of Mechanical Engineering,
Syed Hashim College of Science &
Technology, Pregnapur, Medak District.

Mr. S.S. Mahmood
Associate Professor,
Dept of Mechanical Engineering,
Syed Hashim College of Science &
Technology, Pregnapur, Medak District.

Abstract:

wind turbine rotor blade was designed and developed composites. The baseline design uses e- glass unidirectional fibers in combination with ±45-degree and random mat layers for the skin and spar cap. This project involves developing structural finite element models of the baseline design and carbon hybrid designs with and without twist-bend coupling. All designs were evaluated for a unit load condition and two extreme wind conditions. The unit load condition was used to evaluate the static deflection, twist and twist-coupling parameter. Maximum deflections and strains were determined for the extreme wind conditions. Linear and nonlinear buckling loads were determined for a tip load condition. The results indicate that carbon fibers can be used to produce twist-coupled designs with comparable deflections, strains and buckling loads to the e-glass baseline.

INTRODUCTION:

Wind turbine blades are subject to complex loadings and operational conditions throughout their operating lives. Examples include cyclic loads, varied environmental conditions, parked extreme loads, and operating fatigue loads. Consequently, the design and construction of a cost efficient wind turbine blade that is structurally sound is non-trivial.In general, the weight and cost of the turbine are the keys to making wind energy competitive with other sources of power. According to a recent study2 there is no single component that dominates the turbine cost (rotor, nacelle, drivetrain, power systems and the tower) but it has been identified that minimizing rotor weight has a multiplier effect throughout the system including the foundation.

The weight of the rotor in most of the modern machines is between 37 and 77 % of the total weight of the system1. Thus, based on cost alone, reducing the weight of the blade is an important issue worthy of research. Another factor that plays a very important role is the operational life of the machine. Currently, the industry expects service lives of up to 108 cycles, which translates into roughly 20 years of continuous service2. nalysis takes place outside of NuMAD and results in a series of files containing the solution file, error logs, and other information. These files are automatically generated by ANSYS. The designer/analyst now has a set of files that contain the finite element solutions requested in NuMAD and also all of the model information in an ANSYS format that can be used for further post analysis/processing. If desired, further analysis can be performed without the help of NuMAD.It is important to remember that ANSYS has rules and limitations for the creation and analysis of models. The user is responsible for following good modeling practices and verifying that the elements are being used appropriately. An example is the use of SHELL99 elements with an extremely small radius of curvature. This problem was encountered at the leading edge due to airfoils with small radii, which produced undesirable radius to thickness ratios for the SHELL99 elements. This problem was fixed by replacing the material at the leading edge with a material of equivalent stiffness, but with smaller thickness and higher elastic constants. Another option would have been to create structural cross-sections that were different from the airfoil cross-sections. This option was not used due to the desire to keep an exact geometry model. What this really means is that NuMAD does not prevent users from creating bad models. NuMAD does significantly reduce the time and effort required to produce a blade finite element model.

Based on this project the reduction of modeling time is estimated to be as much as 50 to 60 % compared with the time that would take to create the same model directly in ANSYS. The number of points should also be selected to be an even number and symmetric with respect to the chord line. This produces a model with properly aligned elements and real constant sets (material properties created for the ANSYS model) that will produce a more accurate blade model. Figure 10 shows two models. The left model used a non-symmetric airfoil while the right one used a symmetric airfoil. The different shades represent the real constant sets in ANSYS. Notice the difference in the assignment of real constants to the elements in Figure 10. The left model needs correction because the shades representing the real constants on the left show that the different materials and thickness are not aligned correctly at the transitions shown by the arrows. The right mesh has been properly modeled.
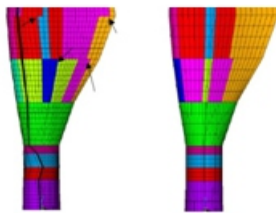

Figure 10.   Real constant variations due to airfoil non symmetry vs. symmetry

For the span-wise direction, geometry was interpolated by NuMAD between stations with airfoil data. The airfoil defining stations are shown in Figure 11. NuMAD assumes that the material definition remains constant between airfoil def ining stations. Some of the ply drops did not coincide exactly with these stations. This problem was especially true near the root sections (STA 0000 to STA 1000) where according to the engineering drawings a large number of plies dropped in a very small length.This problem was resolved by using the closest station to the ply drops and either extending or shortening the layers to make them coincide with the shown stations. For example, if a ply drop occurs at station 900 this layer (or layers) of materials was extended to the next available station, in this case station 1000. This is necessary because NuMAD defines the layers of material starting at the inboard station (900) and uses the same material definition until the next station (1000). Figure 12 shows the graphical interface in NuMAD that allows the user to select the desired circumferential section to which a material previously defined will be assigned.

This approach requires good engineering judgment because some of the layers are shortened or extended spanwise depending on the number of airfoils available. If the designer determines that it would not be acceptable to extend or shorten a given layer to make it coincide with a predefined airfoil, it is possible to define a new station. However, defining a new station is not trivial, and in some cases can create distortions in the model. For the current project, stations were added near the root (stations 400 and 520) because it was determined that the stiffness in the root section might be greatly overestimated if the layers were extended directly from station 278 to station 600.

At this point in the modeling the designer/analyst can assign material properties to each of the sections previously identified and defined. For a composite blade this is done by defining the properties and orientation of each layer that will be part of the laminate and by defining the different laminates that make up the structural cross section. This is when the usefulness of Figure 8 becomes apparent. In NuMAD the user is prompted to divide the airfoil into the number of necessary sections in order to define the structural characteristics of the blade, including spar caps, shear webs, ply drops, etc. Every time there is a ply drop in the circumferential direction there must be a point to coincide with it because a new laminate definition is required. As previously mentioned, not every individual ply drop is captured in the current model. For the NPS-100 twenty laminates (or materials) were created. The information for each of the materials at blade station 1000 summarized in Table 2 is an example of materials definition.

For every station of the blade a table similar to Table 2 and a plot similar to Figure 8 was constructed. These constitute both the circumferential and spanwise variation of properties that are required to effectively create a model in NuMAD. This procedure was followed for the creation of the NPS-100 model in NuMAD. The model contains 17 airfoil definitions (each airfoil with 44 points) and is divided into 10 sections in the circumferential direction designated I thru V for the high and low pressure sides (also see Figure A-1). Figure 13 shows station 2200 as it was defined in the final model. The different shades of gray circumferentially denote a different material definition. Figure 14 shows the corresponding portion of the ANSYS model.
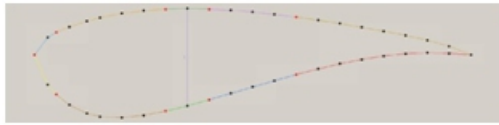
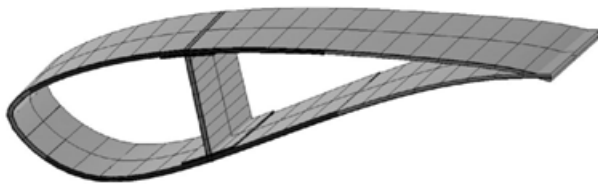Figure 13. Blade station 2200 as defined in NuMAD

Figure 14. Blade station 2200 ANSYS model

Using this same modeling approach, three more models were created using NuMAD.

• 0 degrees carbon substitution

• 15 degrees carbon substitution

• 20 degrees carbon substitution

All of the models were created by replacing the spar cap axial glass fibers with carbon fibers. Detailed descriptions of these models are included in the next section. Once the model was defined in NuMAD, the static analysis option was selected and the analysis launched. This action establishes a link between NuMAD and the ANSYS finite element model. Figure 15 shows an isometric view of the NPS-100 finite element model.
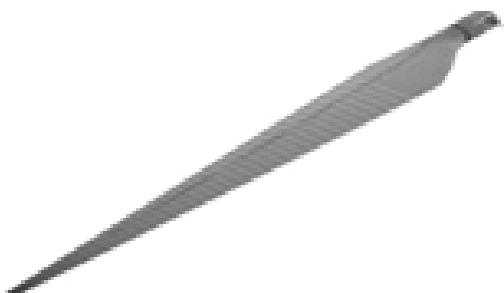

Figure 15. ANSYS finite element model of the NPS-100

The final model consists of 3770 elements and 11156 nodes. As previously mentioned, NuMAD selects by default (from the ANSYS element library) the SHELL99 element. SHELL99 is an 8 node quadratic element that can model up to 250 layers.

More layers can be included via a user input constitutive matrix. The element has six degrees of freedom at each node: translations in the nodal x,y, and z directions and rotations about the nodal x,y, and z axes. More information can be found in Reference 12.

2.3 Modeling of the Hybrid Twist-Coupled Blades:

The main objective of this project is to evaluate the feasibility of implementing the twist-coupled designs into an existing blade. The all-glass NPS-100 prototype blade is the baseline for all comparisons. Twist-coupling can be introduced either geometrically (using blade sweep) or by using unbalanced off axis fibers oriented at an angle θ with respect to the primary loading direction. The off axis fibers result in extensional-shear coupling at the layer level with either twist bend or twist extensional coupling at the blade level. These two types of coupling are depicted in Figure 16. The mirror symmetric lay-up, shown in Figure 16a, produces twist bend coupling.
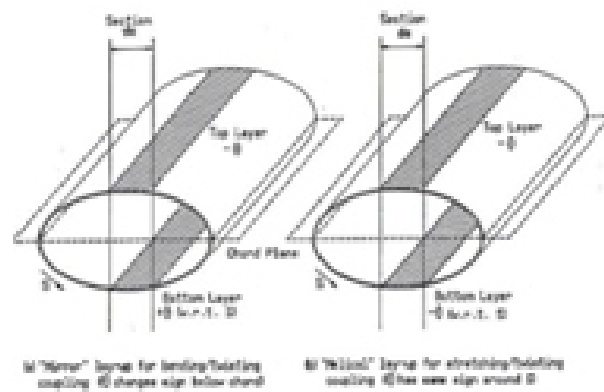

Figure 16. Coupled lay ups (from Karaolis, Reference 3)

For the present study the mirror lay up, Figure 16a, is implemented by changing the C520 unidirectional fibers in the spar caps to off-axis carbon fibers. GEC10 used a similar approach to implement twist-bend coupling for a conventional design. Their results demonstrate that spar cap off-axis carbon fibers are very effective for small amounts of twist. Two key advantages in using this approach are: 1) the same basic manufacturing technology can be employed to produce the blades, and 2) a carbon-hybrid design uses a limited amount of the more expensive carbon material.

NuMAD's capability to assign different orientations to each of the originally defined layers of material was used to define the mirror lay up. The procedure followed was to use the original baseline model and replace the layers of C520 in the spar caps with carbon and then modify the orientation θ of the selected layers. Figure 17 shows one of the element layer stacking sequences generated in ANSYS for the 20-degree carbon substitution on the low-pressure side of the blade.

As shown in Figure 18, the maximum spar cap axial stiffness coefficient is for the carbon at θ = 0°; whereas, the maximum spar cap twist-coupling coefficient is for the carbon at θ = 20°. It should be noted that the axial stiffness at θ = 15° is slightly higher than the value at θ = 20°, and the twist-coupling coefficient is virtually the same for these two cases. This indicates that the design with θ = 15° could be a better design since it produces more axial stiffness with the same level of coupling.

For preliminary designs, it was assumed that a value of the spar cap axial stiffness coefficient equal to the baseline axial stiffness coefficient would yield satisfactory design margins. Based on this assumption the spar cap C520 thickness was scaled down for the carbon designs. The required carbon C520 thickness values are shown in Figure 20. Consistent with the results shown in Figure 18, the minimum required spar cap C520 stiffness is for the carbon at θ = 0°.

1. The mass distribution calculation was based solely on the surface area calculations and the assumed material densities; these calculations are not based on the F.E model.

2. The fiber volume of the materials is assumed to be 50%.

3. The carbon substitution only took place outboard of station 800.

4. There are no material substitutions in the shear web, and the shear web, for weight calculations, was assumed to start at station 1000 and end at station 7200.

Figure 21 shows the spanwise variation in surface area. Figures 22 and 23 show the resulting weight approximation.

3.2 Stiffness Results:

Based on the assumption that an equivalent value of the spar cap axial stiffness coefficient would yield satisfactory results, models I through IV were developed following the information shown in Figure 20. At this stage the main goal was to obtain a flapwise bending stiffness (EI) for models II through IV that was the same as the baseline. The results obtained by the finite element analysis for the baseline were compared with preliminary unpublished data that were provided by Mike Zuteck, of MDZ Consulting. As indicated in the following section, Mike Zuteck's estimated stiffness and the finite element determined stiffness are in good agreement in the flapwise direction. The models were also used to evaluate the edgewise and torsional stiffness of the blade. For this set of analyses the blade was treated as a cantilever beam with all of the model degrees of freedom constrained at the root section.

3.2.1 Flapwise Rigidity:

To study the flapwise rigidity, two 250 lb loads were applied to the tip of the blade as shown in Figure 24.

Figure 24. Application of a 500 lb flapwise tip load

3.2.2 Edgewise Rigidity:

For the calculation of the edgewise rigidity two 250 lb loads were applied to the tip of the blade as shown in Figure 27.
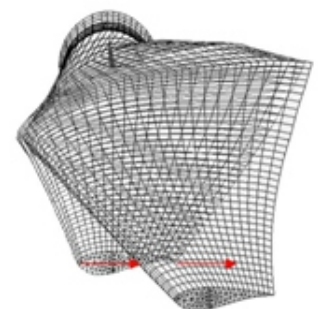

Figure 27.Application of a 500 lb edgewise tip load

As in the previous section, the results from the deformed shape were recorded and both the angle of bending with respect to the global z axis (longitudinal) and the bending rate per unit length were calculated. Equation (5) was used for the approximate values of edgewise bending stiffness. The results are presented in Figures 28 and 29.

LINEAR BUCKLING

A plate buckles when the linear bending stiffness can not resist the bending produced by in plane compression loads. The corresponding equilibrium configuration must be determined using nonlinear analysis that can account for the geometrically nonlinear stiffness. The transition from the stable flat panel to the deflected buckled panel generally occurs with a small change in load. The average load at which this transition occurs can be approximately determined using a linear buckling analysis14.As in the case of the vibration problem, linear buckling analysis can be reduced to the solution of an eigenvalue problem:

$$([K] + \lambda[S])\{u\} = \{0\} \quad (13)$$

where [K] is the stiffness matrix, [S] is the geometric stiffness matrix, λ is the buckling load scale factor and {u} is the buckling mode shape vector. The geometric stiffness matrix includes initial stresses that are determined from a linear static analysis.ANSYS uses an iterative technique to find a set of buckling eigenvalues and eigenvectors that satisfy Eq. (13). NuMAD has the capability of setting up the linear buckling analysis based on an applied tip load. Figures 40 through 43 show the ANSYS plots of the out-of-plane displacement component and the buckling load value in Newtons (FREQ=Buckling Load) on the upper left side.
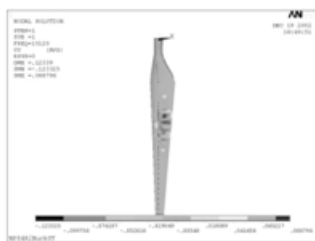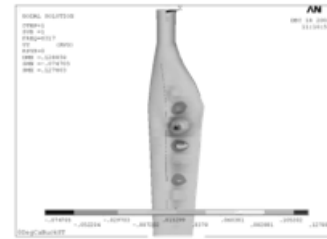

Figure 40.   NPS-100 baseline linear buckling

CONCLUSIONS:

The purpose of this study was to compare the baseline e-glass design of the Northern Power Systems NPS-100 prototype wind turbine rotor blade with twist-coupled, carbon-hybrid designs. Twist-coupled carbon designs were obtained by changing the unidirectional fibers in the spar caps to off-axis carbon fibers. The assumption was made that the carbon blades should deflect the same amount as the baseline for the unit load condition. In order to investigate these issues, four ANSYS finite element models were created using NuMAD. The deflection results show that similar flapwise deflections were obtained for all of the carbon-hybrid designs.

The stiffer carbon fibers resulted in a reduction of the spar cap thickness: 43% of the baseline thickness for the 0-degree carbon, 63% for the 15-degree carbon, and 82% for the 20-degree carbon. These reductions in spar cap thickness also had an impact on the buckling loads. A decrease in the linear buckling load of 58% occurred for the 0-degree carbon design with 29% for the 15-degree carbon design. The 20-degree carbon design had approximately the same linear buckling load as the baseline design. This can be explained by the fact that the buckling load is proportional to the spar cap bending stiffness which depends on the cube of the thickness. It is interesting to notice that although the 20-degree carbon design is 82% of the original thickness, the buckling load remains close to the baseline buckling load. For a complex design the buckling is obviously dependent on other design details that require further investigation.

REFERENCES:

1.D. Ancona, J. McVeigh, "Wind Turbine-Materials and Manufacturing Fact Sheet" OIT-DOE Web site: http://www.oit.doe.gov/bestpractices/energymatters/emextra /pdfs/wind_materials.pdf

2.D.A. Spera, "Fatigue Design in Wind Turbines", Wind Turbine Technology-Fundamental Concepts in Wind turbine Engineering, ASME Press,1998

3.N. M. Karaolis, P. J. Mussgrove, and G. Jeronimidis G, "Active and Passive Aeroelastic Power Control using Asymmetric Fibre Reinforced Laminates for Wind Turbine Blades," Proc. 10th British Wind Energy Conf., D. J. Milbrow, Ed., London, March 22-24, 1988.

4.D. W. Lobitz, D. J. Laino, "Load Mitigation with Twist-Coupled HAWT Blades," AIAA Paper 99-0033, 1999 ASME Wind Energy Symposium, Reno, NV, January 1999.

5.D. Lobitz, P. Veers, D. Laino, "Performance of Twist-Coupled Blades on Variable Speed Rotors," AIAA 2000-0062, 2000 ASME Wind Energy Symposium, Reno, January 2000.

6.D.W. Lobitz, P.S. Veers, G.R. Eisler, D.J. Laino, P.G. Migliore, and G. Bir, "The Use of Twist-Coupled Blades to Enhance the Performance of Horizontal Axis Wind Turbines," SAND2001-1003, Sandia National Laboratories, Albuquerque, NM, May 2001.

7.C.-H. Ong, S. W. Tsai, "Design, Manufacture, and Testing of a Bend-Twist D-Spar," AIAA paper 99-0025, 1999 ASME Wind Energy Symposium, Reno, NV, Janu